ELSEVIER

PII: S0032-3861(97)00154-7

Polymer Vol. 39 Nos. 6–7, pp. 1415–1427, 1998

0032-3861/97/$17.00+0.00

The crystallization of poly(ethylene oxide) in blends with neat and plasticized poly(vinyl chloride)

J.M. Marentette† and G.R. Brown*
Department of Chemistry, McGill University, 801 Sherbrooke Street West, Montreal, Quebec, Canada H3A 2K6
(Received 27 March 1996; revised 20 January 1997)

This study concerns the morphology and spherulite growth rates of poly(ethylene oxide) (PEO), a semicrystalline polymer, in binary blends with poly(vinyl chloride) (PVC), an amorphous polymer, and in ternary mixtures containing (i) the amorphous polymer and (ii) tricresyl phosphate (TCP), a plasticizer for PVC. It is shown that the determining factor in the slight melting temperature depression observed in PEO/PVC blends by differential scanning calorimetry is the influence of PVC on the crystalline structure of PEO. PVC does not influence the spherulite radial growth rates of PEO, measured using polarized light videomicroscopy, in the accessible temperature range; however, TCP causes a substantial depression in the growth rates. Both additives cause the spherulite structure to become coarser and less birefringent. Unusual radial extinction bands indicate that TCP is incorporated within amorphous fold surfaces of PEO lamellae. Studies using polarized infrared microspectroscopy demonstrate that PVC causes a disordering of the orientation of the crystalline stems of PEO, and induces a higher incidence of the trans planar zig-zag conformation of the PEO chains within spherulites grown in PEO/PVC blends. Epitaxial interaction between PEO and PVC also leads to an increased incidence of the planar zig-zag conformation of the PVC. In contrast, TCP has a minimal effect on the orientation and conformation of PEO. In ternary mixtures containing PEO, PVC and TCP, the plasticization of PVC by TCP drastically reduces the effects of PVC on the microstructure of PEO.

(Keywords: Poly(ethylene oxide); crystallization; blends)

INTRODUCTION

In spite of the potential of plasticizers as additional tools for the control of the crystallization of semicrystalline polymers from the melt in semicrystalline-amorphous polymer blends, very little research to date[1] has compared the crystallization behaviour of a binary semicrystalline-amorphous polymer blend with that of a ternary mixture also containing a low molecular weight plasticizer capable of acting on the amorphous polymer. Among the numerous reported studies of miscible or partially miscible blends of poly(ethylene oxide) (PEO) with an amorphous polymer[1–17], blends with poly(vinyl chloride) (PVC) are of particular interest because PVC does not appear to influence the crystallization kinetics of PEO[16]. In fact, this type of behaviour is characteristic of an immiscible blend[18]. However, the morphology of spherulites grown from these blends is disturbed by the presence of PVC, with spherulite structure becoming coarser with increasing concentration of the amorphous polymer[16], as in the case of other miscible blends[3–5,10–17].

The present study examines the crystallization of PEO from the melt in: (i) binary blends with PVC; (ii) a binary mixture with a low molecular weight plasticizer tricresyl phosphate (TCP), commonly used with PVC in industrial applications; and (iii) ternary mixtures containing both PVC and TCP. Thermal analysis is employed to obtain insight regarding the melting behaviour and to evaluate the extent of miscibility of PEO and PVC. Polarized light microscopy (PLM) is used to observe the crystallization kinetics and morphology of PEO spherulites; while the technique of polarized infrared microspectroscopy (PIRM) is applied to the examination of the orientation of the crystalline stems and the conformation of polymer chains within the spherulites.

EXPERIMENTAL

Sample preparation

The synthesis of monodisperse PEO ($\overline{M_w} = 1.8 \times 10^5$; polydispersity $\overline{M_w}/\overline{M_n} = 1.4$) was described in the preceding paper[19]. The PVC resin (Esso 366, supplied by Les Industries Synergistics Ltèe., St Rémi-de-Napierville, Quebec) was reprecipitated to remove additives and the low molecular weight fraction[20]. The $\overline{M_w}$ and the polydispersity were determined by gel permeation chromatography using polystyrene standards, as 1.1×10^5 and 1.8, respectively[20]. Industrial tricresyl phosphate (90%, Anachemia), consisting predominantly of the meta- and para-tricresyl isomers (90%), was used as received.

Blends of PEO containing 10, 18, 25, 35 and 50 wt% PVC were prepared by solution blending in 1,2-dichloroethane (DCE) at room temperature, under N_2, followed by precipitation in chilled hexanes[20]. Due to the low melting temperature of TCP and the differing solubilities of the liquid plasticizer and the polymers, solution casting from

*To whom correspondence should be addressed. Present address: University of Northern British Columbia, Chemistry Programme, 3333 University Way, Prince George, BC, Canada V2N 4Z9
† Present address: Max Planck Institute for Polymer Research, Ackermannweg 10, Postfach 3148, D-55021 Mainz, Germany

Table 1 Equilibrium melting temperature and heat of fusion data for PEO and the PEO/PVC blends. (The lamellar thickening factor is given by η)

PVC (wt%)	T_m° (°C)	ΔH_{bl} (J g^{-1} blend)	ΔH_{fus} (J g^{-1} of PEO)	Crystallinity[a] (%)	η
0	76 ± 2	168 ± 11	168 ± 11	78 ± 5	3.36 ± 0.03
10	73 ± 4	156 ± 4	173 ± 4	80 ± 2	3.13 ± 0.05
18	72 ± 3	140 ± 3	171 ± 4	79 ± 2	3.25 ± 0.04
25	72 + 7	130 ± 3	173 ± 4	80 ± 2	3.38 ± 0.10
35	72 ± 4	108 ± 1	166 ± 2	77 ± 1	3.07 ± 0.05
50	71 ± 2	82 ± 2	164 ± 4	76 ± 2	3.61 ± 0.03

[a]Where 216 ± 2 J g^{-1} has been taken as the heat of fusion of perfectly crystalline PEO[20,22,23]

DCE was employed instead of solution blending. An excess amount of plasticizer (50 parts by weight per 100 parts of resin) was added to appropriate amounts of PEO, PEO/PVC (82/18), and PEO/PVC (65/35). All of the samples were allowed to air-dry for 3 days before being placed under vacuum at room temperature to dry for 4 weeks prior to crystallization measurements. All of the samples were stored at room temperature under vacuum. Abbreviations of the form PEO/PVC/TCP (wt% PEO/wt% PVC/wt% TCP) will be used to denote the various blends and mixtures.

Differential scanning calorimetry

The melting transitions of PEO in blends with PVC and TCP were determined using a Perkin-Elmer DSC-7 operating in the ambient mode, with rapid cooling provided by a Perkin-Elmer intracooler according to procedures described in the preceding paper[19]. Each sample (weighing 5.0 ± 0.2 mg) was held in the melt at 100°C for 15 min in the DSC, then quenched at a nominal rate of 200°C min^{-1} to a crystallization temperature (T_c) in the range 48–60°C in the case of the PEO/PVC blends, or 40–48°C in the case of the plasticizer mixtures. The sample was maintained at T_c for 24 h or, in the instance of small supercooling, a length of time sufficient to ensure complete crystallization, then heated at 10°C min^{-1} to 100°C.

Polarized light microscopy

Except as specified below, the procedures for the preparation of thin sections, sample premelting, spherulite nucleation, the observation of spherulite morphology, and the measurement of spherulite radial growth rates of pure PEO were as described in the preceding paper[19]. In the case of PEO/PVC blends, the molten sample was cooled from 100°C at 130°C min^{-1} to the selected crystallization temperature in the range 45–56°C; in the case of mixtures containing TCP, the selected crystallization temperature range was 35–48°C. Low temperature nucleation was also carried out for all of the samples[20]. Thin sections of pure PEO were melted and recrystallized up to six times with no effect on the growth rate, but thin sections of the blends and the mixtures were crystallized once only due to the possibility of additive degradation that can result from repeated melting.

The radial growth rates were obtained from spherulites or sectors of spherulites that did not impinge on others during the time span of the measurement. Correlation coefficients ≥ 0.9990 were obtained except for the case of spherulites crystallized from PEO/PVC (50/50), PEO/PVC/TCP (55/12/33) and PEO/PVC/TCP (44/23/33), where irregular, diffuse boundaries resulted in correlation coefficients with a minimum value of 0.990.

Polarized infrared microspectroscopy

Crystalline stem orientation and chain conformation in local areas of spherulitic thin sections were examined using a Perkin-Elmer infrared microscope. The methodology for sample preparation and spectral acquisition were described in the preceding paper[19].

RESULTS AND DISCUSSION

Equilibrium melting temperatures

The Hoffman–Weeks technique, which employs the relation

$$T_m = \frac{1}{\eta}T_c + T_m^\circ\left(1 - \frac{1}{\eta}\right) \quad (1)$$

where η is referred to as the lamellar thickening factor[21], was used to estimate the equilibrium melting temperature, T_m°, of PEO in the various blends. The results listed in *Table 1* demonstrate that T_m° decreases slightly upon addition of PVC. The discrepancy of 2–3°C between these data and the results of Margaritis and Kalfoglou[17] can be attributed to the use of endotherm onset temperatures in the literature calculations instead of peak temperatures. The small depression indicates that at best, PEO and PVC are only slightly miscible in the melt at elevated PVC content, but are likely immiscible over most of the concentration range. Similar small melting temperature depressions observed by Martuscelli for blends that are immiscible in the melt, e.g. isotactic polypropylene (iPP) blended with low density polyethylene[18], were attributed to unspecified kinetic and morphological factors associated with the presence of isolated domains of non-crystallizable material in the melt. The addition of PVC to PEO exerts a negligible effect on the degree of crystallinity of PEO, as demonstrated by the results listed in *Table 1*.

To further investigate the question of miscibility, the data were analysed according to the Flory–Huggins equation[24–26]:

$$\frac{1}{T_{m,bl}^\circ} - \frac{1}{T_m^\circ} = \frac{-RV_2}{(\Delta H_f^\circ)V_1}\chi_{12}(1-\nu_2)^2 \quad (2)$$

where R is the ideal gas constant, V_i is the molar volume of a repeat unit, ν_i is the volume fraction of a polymer in the blend, and χ_{12} is the thermodynamic interaction parameter that describes the nature and the degree of the interaction between components (1) and (2), the amorphous and the crystalline polymers, respectively. The resultant Flory–Huggins plot was distinctly curved, as reported previously[17]. Others have taken this to be an indication of limited miscibility at PVC concentrations > 35%[16,17,27].

The Hoffman–Weeks plots for the blends containing TCP are shown in *Figure 1*. As a result of a substantial depression of the crystallization rate of PEO in the plasticizer mixtures (shown below), the T_c range used for these samples was 41–47°C, rather than 49–59°C as for the

PEO/PVC blends. The derived values of $T_m°$ are given in *Table 2*. The rather large experimental uncertainties are due to substantial scatter in the data; they do not arise from curvature due to the temperature dependence of η. This scatter reflects a major problem that is encountered in the thermal analysis of blends containing a low molecular weight liquid: the maintenance of uniform geometry and dispersion within a given sample and among different samples. The data for the PEO/PVC/TCP (44/23/33) blend, in particular, show considerable scatter and the $T_m°$ value obtained from the least-squares treatment appears to be an underestimate, so that the actual value may be closer to 70°C. Within the experimental uncertainty the values of $T_m°$ derived for the ternary mixtures cannot be distinguished from those for the pure polymer or the blends. These results suggest that PEO and TCP are immiscible, or only partially miscible, in the melt. The degree of crystallinity of PEO, also listed in *Table 2*, is not significantly affected by the addition of plasticizer.

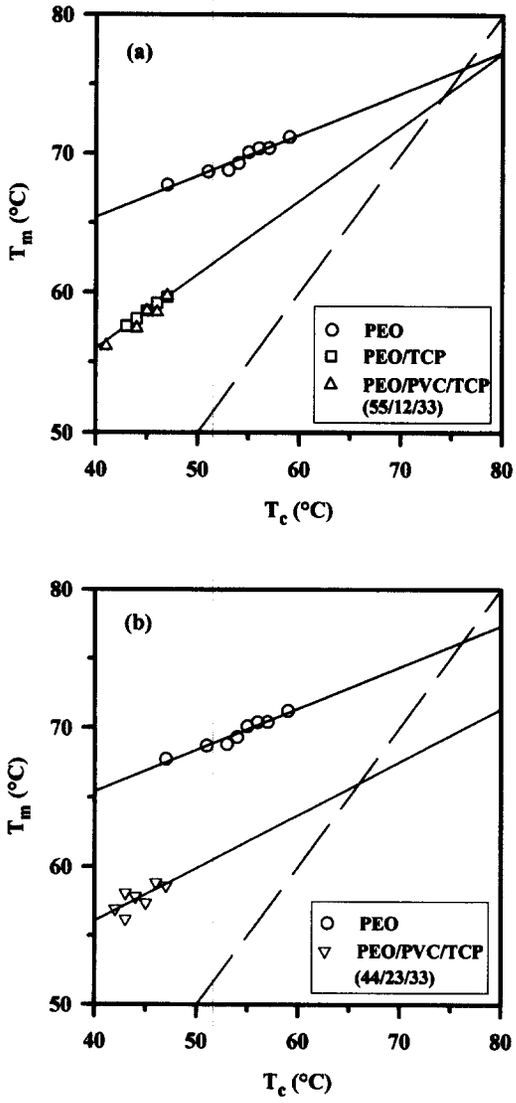

Figure 1 Hoffman–Weeks plots for PEO and TCP mixtures: (a) PEO/TCP (with regression line) and PEO/PVC/TCP (55/12/33) (regression line not shown); (b) PEO/PVC/TCP (44/23/33)

As shown in *Table 2*, the value of η obtained for PEO/PVC/TCP (55/12/33) is similar to that obtained for PEO/TCP; while that obtained for PEO/PVC/TCP (44/23/33) is considerably larger. In any event, it appears that the plasticizer suppresses lamellar thickening in the ternary mixtures as well as in the PEO/TCP mixture. Rejection of the plasticizer molecules by the crystalline PEO leads to an accumulation of these small molecules in interlamellar, interfibrillar and interspherulitic regions. Interactions between the amorphous fold surfaces of PEO and the rejected TCP molecules impede the thickening process.

Spherulite morphology

Spherulites grown in these blends exhibit a gradual coarsening in structure, blurring of the Maltese cross extinction pattern, and diminishing luminescence with increasing PVC content, as shown in *Figure 2*. This results from a substantial decrease in the anisotropy of the crystalline structure at the level of the fibrils. The nucleation density also increases with increasing PVC content, as shown by the data for $T_c = 49°C$ in *Figure 3*.

Photomicrographs of the TCP mixtures at 100°C (*Figure 4*) reveal that PVC is present in larger aggregates in PEO/PVC/TCP (55/12/23) than in the PEO/PVC blend, indicating that TCP preferentially solubilizes the PVC and interferes with the dispersion of PVC in the PEO melt. The aggregation in PEO/PVC/TCP (44/23/33), where there is less plasticizer present relative to the amount of PVC, is more uniform in texture than in the other ternary mixture, but appears more opaque. The T_g for a 50:50 mixture of PVC and TCP is expected to be *ca.* −22°C[28] so the PVC is rubber-like and flexible in these ternary mixtures. As shown in *Figure 3*, plasticization of PVC by TCP leads to the suppression of the influence of PVC on the primary nucleation of PEO.

For consistency, the spherulites shown in *Figure 5* were photographed at temperatures where nucleation occurs readily and the spherulite growth rate is similar to that of PEO in the PEO/PVC blends, i.e., at 40 and 38°C for PEO/TCP and the ternary mixtures, respectively. The morphology of individual spherulites grown from the TCP mixtures is similar to that of spherulites grown from PEO/PVC blends of similar weight percent of non-crystallizing material, with the exception of some evidence of irregular tangential extinction marks. In fact, crystallization at temperatures a few degrees below the selected temperatures reveals the incidence of broad tangential banding, as shown in *Figure 6*(a), a feature that is not seen in spherulites grown from either pure PEO or PEO/PVC blends

Table 2 Equilibrium melting temperature and heat of fusion data for PEO and TCP plasticizer mixtures

PVC (%)	TCP (%)	$T_m°$ (°C)	ΔH_{bl} (J g^{-1} blend)	ΔH_{fus} (J g^{-1} of PEO)	Crystallinity[a] (%)	η
0	0	76 + 2	168 ± 11	168 ± 11	78 ± 5	3.36 ± 0.03
0	33	74 ± 1	105 ± 3	158 ± 4	73 ± 2	1.88 ± 0.01
12	33	76 ± 9	87 ± 3	159 ± 6	74 ± 3	1.73 ± 0.08
23	33	66 ± 11	70 ± 5	161 ± 11	75 ± 5	2.62 ± 0.16

[a]Where 216 ± 2 J g^{-1} has been taken as the heat of fusion of perfectly crystalline PEO[20,22,23]

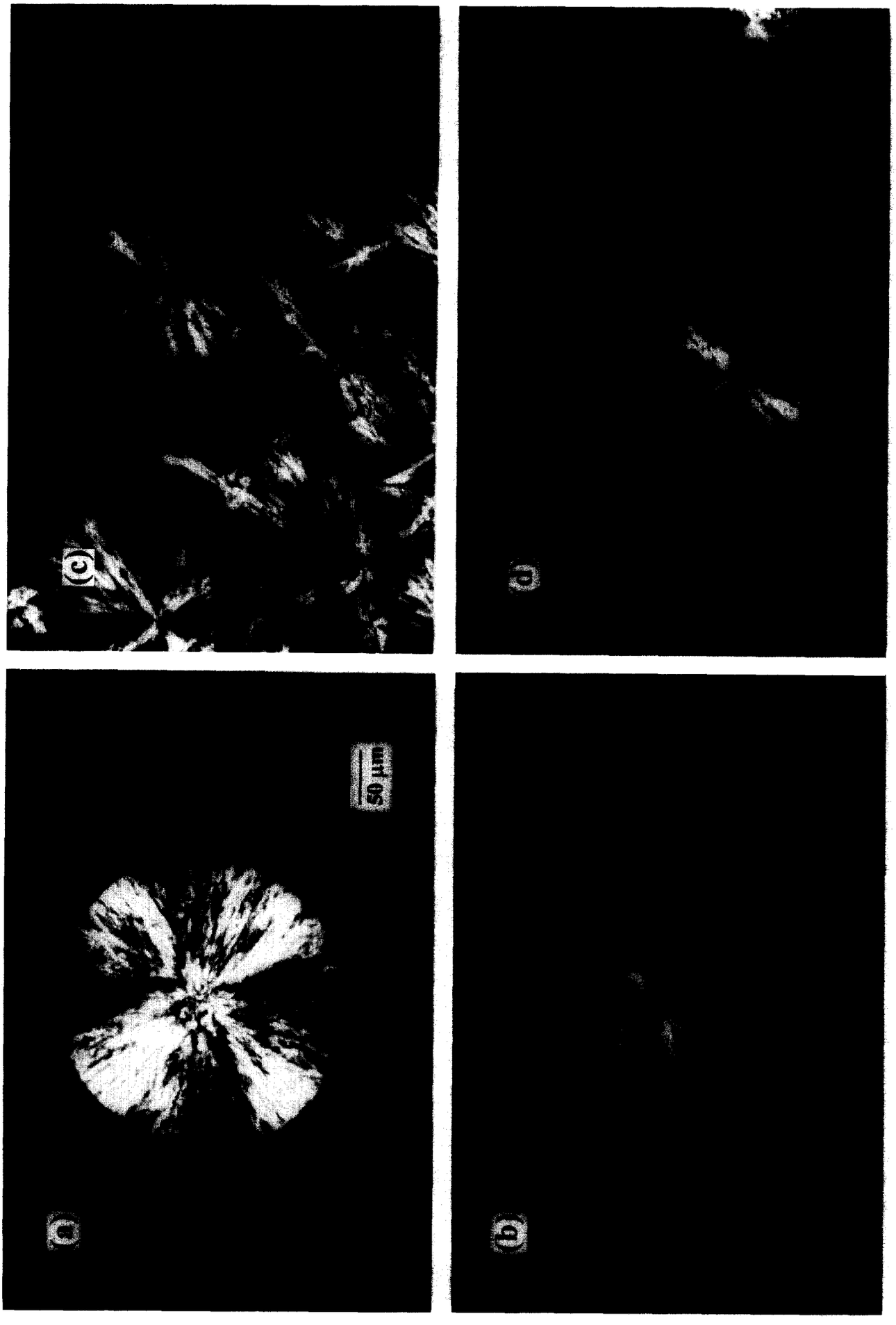

Figure 2 Variation of spherulite morphology with PEO/PVC blend composition, $T_c = 49°C$: (a) PEO, (b) PEO/PVC (82/18), (c) PEO/PVC (65/35), (d) PEO/PVC (50/50)

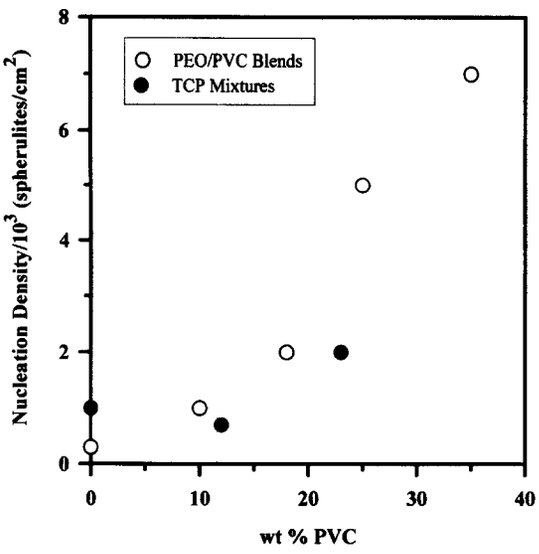

Figure 3 Spherulite nucleation density as a function of PVC content

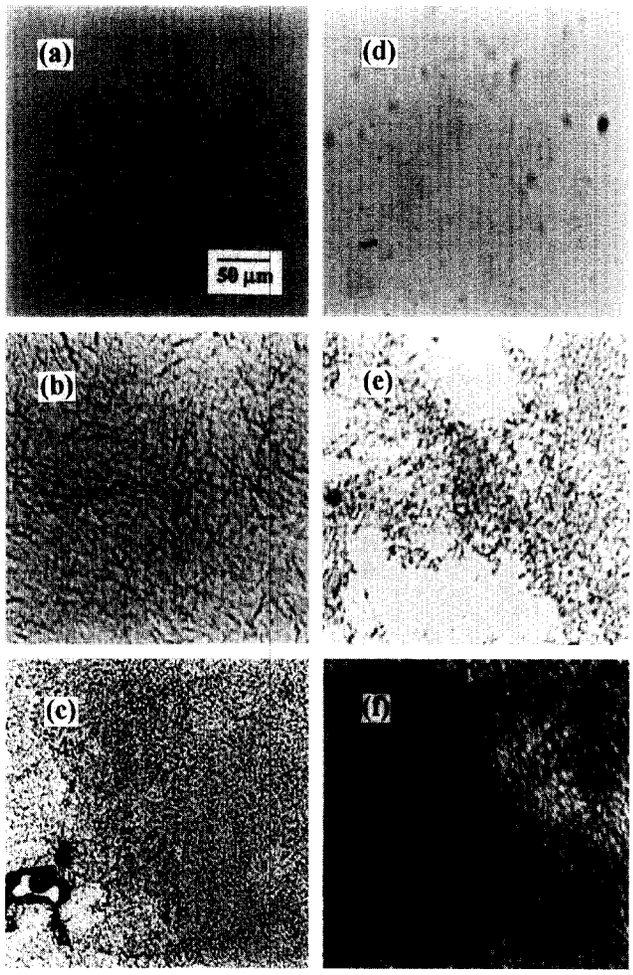

Figure 4 Melt morphology at 100°C: (a) PEO/PVC (82/18), (b) PEO/PVC (65/35), (c) PEO/PVC (50/50), (d) PEO/TCP, (e) PEO/PVC/TCP (55/12/33), (f) PEO/PVC/TCP (44/23/33)

at equivalent or more rapid growth rates, in the T_c range studied. The bands become more irregular and diffuse with the addition of PVC, and at 23% PVC [*Figure 6*(c)] they have all but disappeared, i.e., the introduction of PVC disrupts or diffuses the effect of TCP.

Such extinction patterns are generally attributed to the

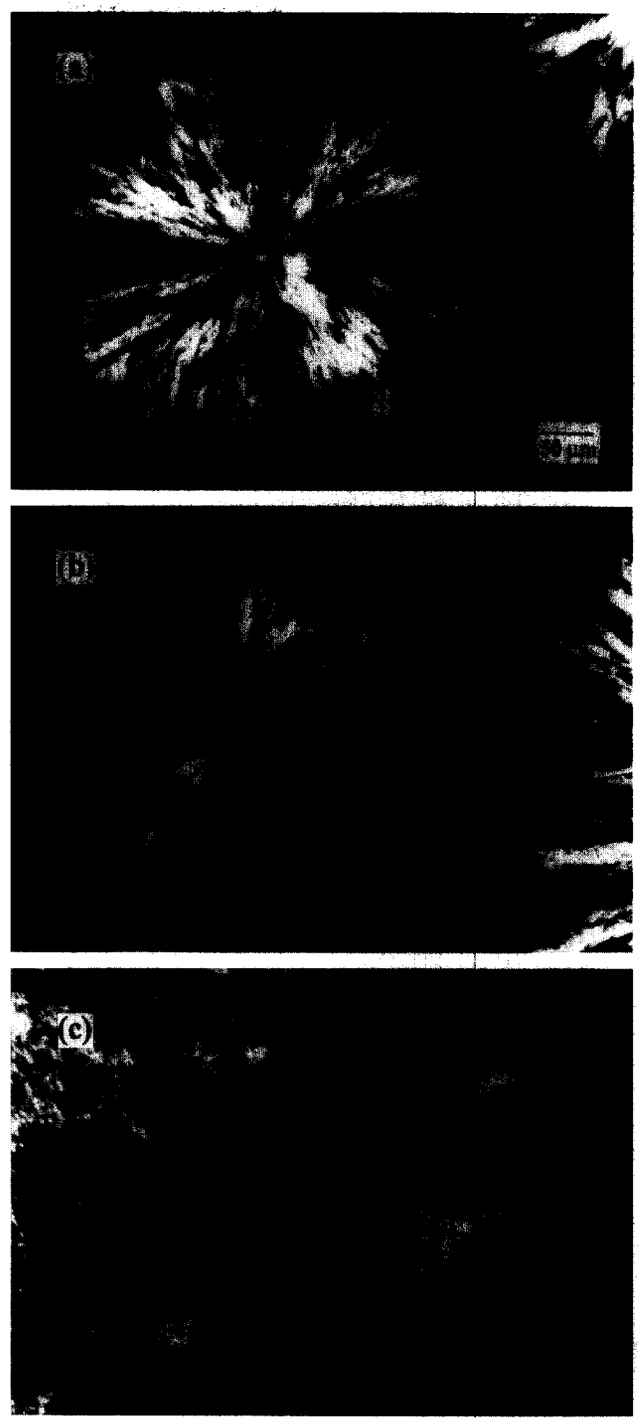

Figure 5 Spherulite morphology in TCP mixtures: (a) PEO/TCP (67/33), $T_c = 40$°C, (b) PEO/PVC/TCP (55/12/33), $T_c = 38$°C, (c) PEO/PVC/TCP, $T_c = 38$°C

radial twisting of fibrils[29]. Although very diffuse banding in spherulites of PEO grown from the pure melt has been noted previously in the literature[30], distinct, tangential extinction patterns have only been reported in instances where PEO crystallized in the form of a stoichiometric complex with a low molecular weight material such as resorcinol[31] or p-nitrophenol[32]. These complexes also exhibited drastically different melting behaviour and crystallization kinetics from pure PEO. Keith *et al.*[33] also observed distinct bands in spherulites of poly(ϵ-caprolactone) (PCL) grown from the melt in miscible blends with PVC, in a temperature range where PCL does not normally exhibit banding. They attributed these effects to the accumulation of diluent in

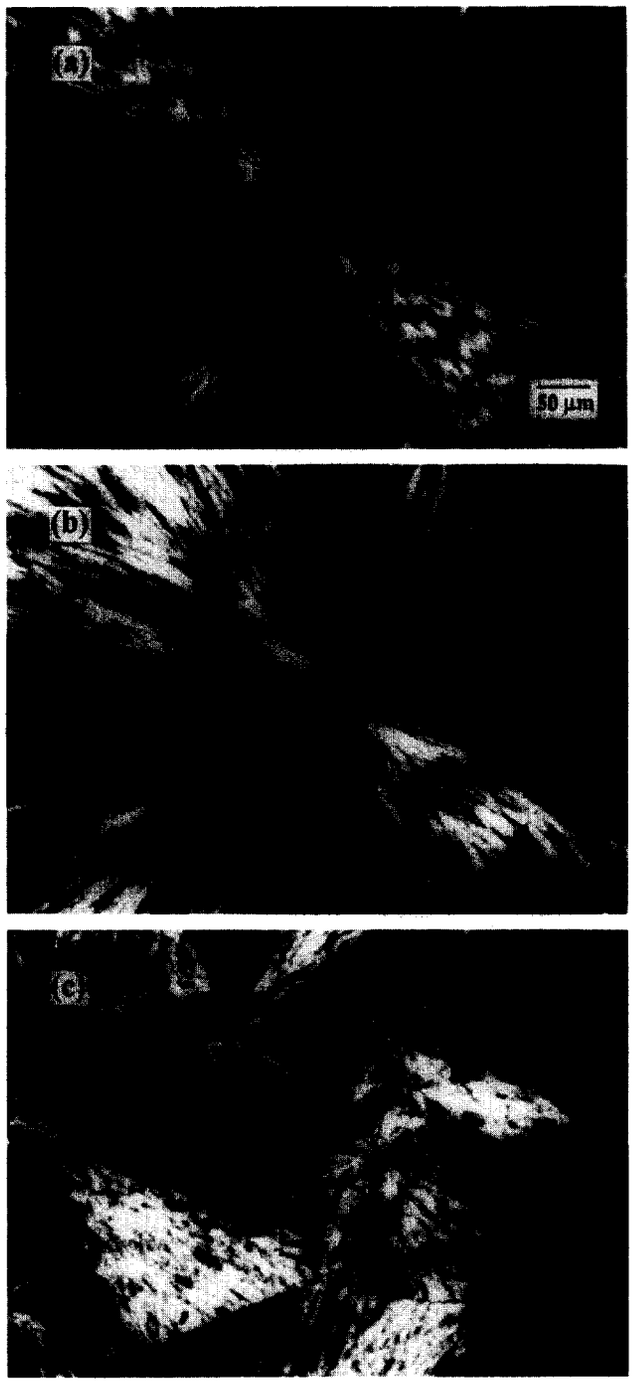

Figure 6 Banding in spherulites in TCP mixtures at 35°C: (a) PEO/TCP (67/33), (b) PEO/PVC/TCP (55/12/33), (c) PEO/PVC/TCP (44/23/33)

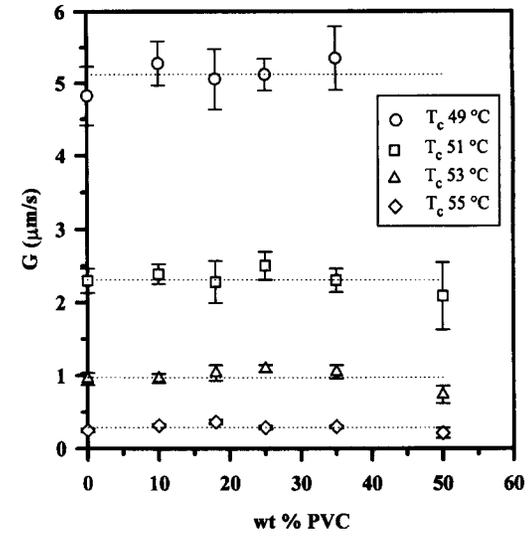

Figure 7 Spherulite radial growth rate as a function of PEO/PVC blend composition at various T_c (the average growth rate is shown by a dotted line)

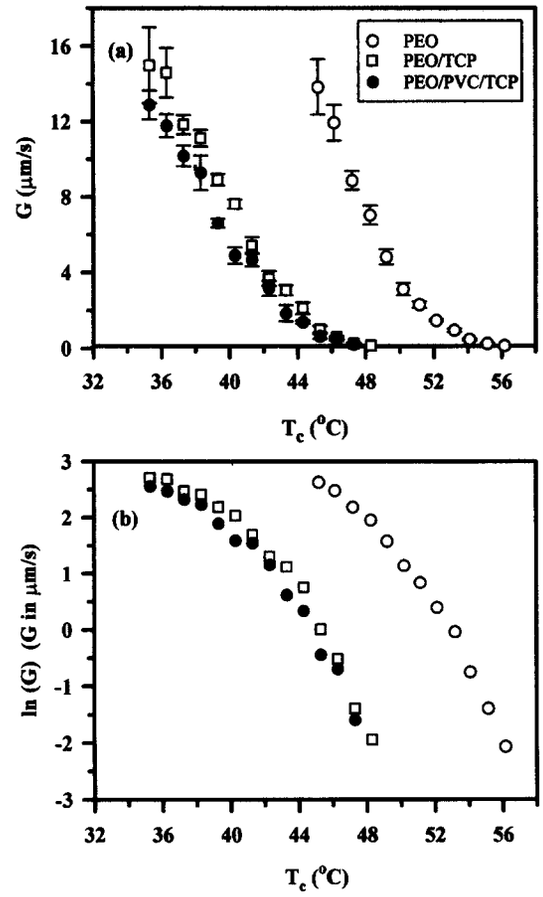

Figure 8 (a) Spherulite radial growth rate as a function of T_c in mixtures containing TCP, and (b) logarithmic growth rate plots (the data for pure PEO are shown for reference)

interlamellar regions of spherulites and to the resultant adsorption of diluent molecules both on the growth faces and on the fold surfaces of the crystals[33,34]. Analogously, the results obtained in the present study indicate that some of the TCP molecules must be incorporated between the radially stacking lamellae during spherulite growth.

Crystallization kinetics

The radial growth rates of PEO spherulites as a function of blend composition are plotted in *Figure 7*. Due to the enhanced nucleation density in these blends, growth rate data could not be obtained at $T_c < 49$°C. In spite of the morphological changes undergone by spherulites of PEO upon addition of PVC, within the experimental uncertainty these growth rates are identical to those of the pure polymer, confirming the observations of Iragorri *et al.*[16] If PEO and PVC exhibit limited miscibility in the melt, as implied by the DSC results, this miscibility has an insignificant effect on the crystallization kinetics.

In contrast to the PEO/PVC blends, the accessible portions of the growth rate curves of spherulites grown in

PEO/TCP (67/33) and PEO/PVC/TCP (55/12/33), shown in *Figure 8*(a), are substantially displaced to lower temperatures relative to the curve for pure PEO. The growth rates for the ternary mixtures are very similar to those for PEO/TCP; and data for PEO/PVC/TCP (44/23/33) are coincident with corresponding data for the ternary mixture of lower PVC content. The effect of TCP on the crystallization kinetics of PEO is diminished in the ternary mixtures by preferential mixing of TCP with PVC such that the amount of plasticizer available to mix with molten PEO is reduced. The logarithmic growth rate plots in *Figure 8*(b) reveals cusps at 42 and 40°C for PEO/TCP and PEO/PVC/TCP (55/12/33), respectively, that resemble the slight cusp observed at 51°C in the plot obtained for pure PEO[19].

Various attempts have been made to devise equations that describe the crystallization of semicrystalline polymers in blends, all of which employed the Hoffman–Lauritzen equation[35–37], or the earlier Turnbull–Fisher equation[38], as a starting point[20,39–42]. However, the radial growth rates of PEO spherulites in the various PVC blends appear to be unperturbed by the presence of the non-crystalizing polymer and none of the available growth rate equations lends itself to the interpretation of growth rate data for ternary mixtures. Therefore, as a first approximation the data were analysed with the original Hoffman–Lauritzen equation:

$$G = G_0 \exp\left[\frac{-U^*}{R(T_c - T_\infty)}\right] \exp\left[\frac{-K_g}{T_c(\Delta T)f}\right] \quad (3)$$

where G_0 is a pre-exponential factor, U^* is the activation energy for reptation in the melt, R is the ideal gas constant, T_∞ is the temperature of cessation of molecular motion (often taken as $T_g - 30$K), and ΔT is the supercooling, $T_m - T_c$[35–37]. The dimensionless correction factor, f, is equal to $2T_c/(T_m^\circ + T_c)$, and is intended to compensate for the decreasing heat of fusion with decreasing T_c. The nucleation constant is given by

$$K_g = \frac{2jb_0\sigma\sigma_e T_m^\circ}{k(\Delta H_f^0)} \quad (4)$$

where b_0 is the crystalline molecular thickness in the growth direction, σ is the lateral surface interfacial free energy, σ_e is the fold surface interfacial free energy, and ΔH_f^0 is the heat of fusion per unit volume of monomer units[35–37]. The parameter j is equal to 2 in regimes I and III, and 1 in regime II.

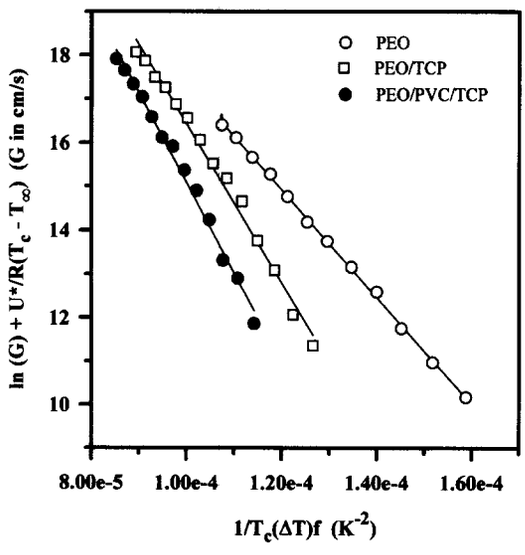

Figure 9 Hoffman–Lauritzen plots for spherulites grown in TCP mixtures (the data for PEO are shown for reference)

The plots for PEO/TCP and PEO/PVC/TCP (55/12/33) in *Figure 9* are linear with correlation coefficients of 0.9957 and 0.9960, respectively. The values of T_m° that were employed are those obtained by the Hoffman–Weeks method, i.e., 74 and 76°C for PEO/TCP and PEO/PVC/TCP (55/12/33), respectively. The effect of additives on the true T_g of PEO could not be determined due to nucleation of PEO by the additives during quenching[20]. Because growth rate data cannot be fitted to equation (3) with both T_∞ and U^* as variable parameters, and without any available data on the transport-controlled side of the growth rate–temperature curve, the values of T_∞ and U^* used were those of pure PEO ($T_g - 30$K) or −108°C and 23.9 kJ mol^{-1}, respectively[19]. In these calculations errors in the estimate of the values for T_∞ and U^* are expected to influence the resultant values of G_0, but will have a minimal effect on the nucleation term[35].

Knowledge of the values of b_0 and ΔH_f^0 and the slope of a plot of ln (G) + $[U^*/R(T_c - T_\infty)]$ as a function of $1/T_c(\Delta T)f$ permits calculation of $\sigma\sigma_e$ for a given polymer and regime. The Lauritzen Z-test[35,37,43] indicates that these data all lie within regime III, as is the case of pure PEO[19]. An estimation of σ, and therefore σ_e, can be obtained by use of the empirical relation

$$\alpha_{LH} = \frac{\sigma}{(\Delta H_f^0)(a_0 b_0)^{1/2}} \quad (5)$$

where $a_0 b_0$ is the cross-sectional area of the polymer[37]. The parameter α_{LH} is an empirical parameter that has been estimated to be equal to 0.1 for most linear polyolefins[37]. The work of chain folding, q, can then be estimated using the following relation:

$$q = 2a_0 b_0 \sigma_e \quad (6)$$

Equations (4)–(6) were used to estimate $\sigma\sigma_e$, σ_e and q. The values of a_0, b_0, ΔH_f^0, α_{LH} and σ were those used in previous calculations for pure PEO[19]: 4.62 Å, 4.62 Å[44], 2.66 × 10^9 erg cm^{-3} (216 ± 2 J g^{-1})[22,23], 0.1[37] and 12.3 erg cm^{-2} [19], respectively. The results listed in *Table 3* show that, other parameters remaining constant, the decrease in G reflects an increase in $\sigma\sigma_e$.

Assuming that σ remains constant at 12.3 erg cm^{-2}, then

Table 3 Nucleation constant, surface interfacial free energies, and work of chain folding in PEO spherulites crystallized from PEO, PEO/TCP (67/33) and PEO/PVC/TCP (55/12/33)

Sample	$K_g \times 10^{-5}$ (K^2)	$\sigma\sigma_e$ (erg^2 cm^{-4})	σ_e (erg cm^{-2})	q (kJ mol^{-1})
PEO	1.22 ± 0.01	697 ± 70	57 ± 6	15 ± 2
PEO/TCP	1.81 ± 0.05	1038 ± 104	84 ± 8	22 ± 3
PEO/PVC/TCP[a]	2.05 ± 0.06	1170 + 117	95 ± 10	25 ± 3

[a]The results for PEO/PVC/TCP (44/23/33) are identical with those for the mixture with the lower PVC content

σ_e increases when TCP is added to PEO, indicating that TCP causes an unfavourable alteration of the spherulite fold surface. The entropy increase resulting from the inclusion of the small TCP molecules in the fold surface is expected to outweigh any positive enthalpic contribution that could result. A study of the crystallization of miscible mixtures of iPP and dotriacontane ($C_{32}H_{66}$), in the composition range 10–100% iPP[45] is the only instance where $\sigma\sigma_e$ has been noted to increase relative to the value for the pure polymer. However, the value of T_m° employed in the analysis of radial growth rate data by the Hoffman–Lauritzen equation was the value for pure iPP[45]. The unexpected increase in $\sigma\sigma_e$ observed in the present study, combined with the depression in the spherulite growth rates, strongly suggests that the estimates of T_m° for PEO/TCP and PEO/PVC/TCP obtained by DSC are, in fact, overestimates of the actual values. It is possible that the noted interference of TCP in the lamellar thickening process of PEO precludes an accurate determination of the T_m° of PEO in the plasticizer mixtures by the Hoffman–Weeks method. If $\sigma\sigma_e$ is assumed to be unchanged relative to pure PEO, then the values of T_m° of these mixtures should be lower than the reported values. In the case of PEO/TCP, a value of 697 erg^2 cm^{-4} for $\sigma\sigma_e$ yields a T_m° of 69°C, while in the case of PEO/PVC/TCP (55/12/33), T_m° will be slightly lower.

The best fits to the data for the ternary mixtures shown in *Figure 9* indicate a small degree of curvature. In addition a cusp is apparent in each of the plots in *Figure 8*(b), at 42 and 40°C for PEO/TCP and PEO/PVC/TCP (55/12/33), respectively. The cusp is more pronounced in the case of the temary mixture. For PEO/TCP the ratio of the slope of the low-temperature segment (35–42°C) to that of the high-temperature segment (43–48°C) is 0.72; a similar value is obtained for the ternary mixture. If a lower value of T_m° for PEO/TCP, such as 69°C, is employed in the Hoffman–Lauritzen plot, then the corresponding slope ratio is 0.78. Again, the plot is characterized by a slight degree of curvature, but it is unlikely that this results from a regime transition. More probably it reflects the temperature-dependence of $\sigma\sigma_e$. With decreasing T_c more TCP molecules are entrapped in interlamellar regions, so the entropy of the fold surface increases and $\sigma\sigma_e$ decreases, thereby causing a decrease in K_g. In fact, a decrease in K_g at lower temperatures is the trend that has been observed for these samples.

The growth rate data for PEO/TCP were examined in further detail by constructing a series of Hoffman–Lauritzen plots for various values of T_m°. Then the coefficient of determination (r^2) was maximized with respect to the value of T_m° for the data in the T_c range above the cusp, and for the data in the T_c range below the cusp, with T_∞ and U^* constant. As in the case of pure PEO[19], fits to the two segments yielded different values of T_m°: 54°C for the low-temperature segment, and 75°C for the high-temperature segment (correlation coefficients 0.9991 and 0.9980, respectively). A value of 54°C is a significant underestimate of T_m° because crystalization can be observed at this temperature; while 75°C agrees with the result of the Hoffman–Weeks method. The agreement between the latter value and the Hoffman–Weeks result confirms that the suppression of lamellar thickening observed in bulk samples also occurs in thin sections. If a (010)–(120) growth face transition occurs in mixtures containing TCP, as in the case of pure PEO[19], then it is possible that the determination of two distinct values for T_m° by this method reflects the two different melting temperatures characteristic of (010) and (120) growth, as postulated for pure PEO[19].

Crystalline microstructure

In a previous paper[19], we demonstrated the utility of PIRM for the examination of the orientation of the crystalline stems in local areas of PEO spherulites in thin section. That study was based on the determination of the dichroic ratio, R, defined as

$$R = \frac{A_\parallel}{A_\perp} \tag{7}$$

where the subscripts $\parallel$ and $\perp$ denote parallel and perpendicular orientation relative to the reference direction, respectively, to describe the degree of sample orientation. For drawn samples the parallel direction is taken to be the draw direction, i.e., the direction of the polymer chain axes, and the perpendicular direction lies perpendicular to the chain axes. In the present study of spherulite structure, a spectrum acquired with the infrared polarizer oriented parallel to the spherulite radius is referred to as a 'perpendicular spectrum'; similarly a spectrum acquired with the polarizer oriented along the tangential direction of the spherulite is referred to as a 'parallel spectrum'. Because the parallel direction does not coincide with the length of the chain axes, the magnitude of the dichroism observed in spherulitic thin sections is less than that observed in oriented samples, such as drawn fibres, composed of the same material. However, spherulitic dichroic ratio measurements provide a measure of the degree and nature of the orientation found in sub-spherulitic structure. This technique permitted confirmation of the (010)–(120) growth face transformation in PEO[19].

In general, PEO crystallizes in the form of a distorted 7_2 helix in a monoclinic unit cell[44], but a chain-extended planar zig-zag conformation in a triclinic unit cell has also been observed in stretched or wet samples[46] and in miscible blends with PMMA[47,48]. A previous IR study of solution-cast PEO/PMMA blends reported a simplification of the spectrum of PEO in the presence of amorphous PMMA, which was taken to be an indication of a change in the conformation of the crystalline chains from the complex, distorted 7_2 helical structure to a more symmetrical conformation, such as the planar zig-zag form[47]. According to our previous dichroism assignments[19] the helical modes of PEO[47] are all perpendicular (i.e., radial in terms of spherulite geometry) while the planar zig-zag modes[47] are all parallel (i.e., tangential); therefore any change in the population distribution of these two conformations also influences the dichroism of PEO.

The values of the absorbance (A) at 1468, 1455, 1360, 1344, 1281, 1243, 1062, 965, 947 and 843 cm^{-1} were determined for each set of parallel and perpendicular spectra. The average dichroic ratio (R) at each wavenumber and the average of each of the relevant peak ratios was calculated for a given sample and crystallization temperature. The spectral pair exhibiting results closest to the average results for a given sample was then used as the starting pair for difference spectroscopy. The contributions from TCP, PVC and amorphous PEO were removed, where applicable, from the starting pairs of spectra to reveal the spectra of purely crystaline PEO, for which the dichroic ratios and peak ratios were determined. The values of the absorbance were < 1.0, with the exception of some values obtained at 1344, 1281 and 843 cm^{-1}, where A was ≥ 1.0, but < 1.5.

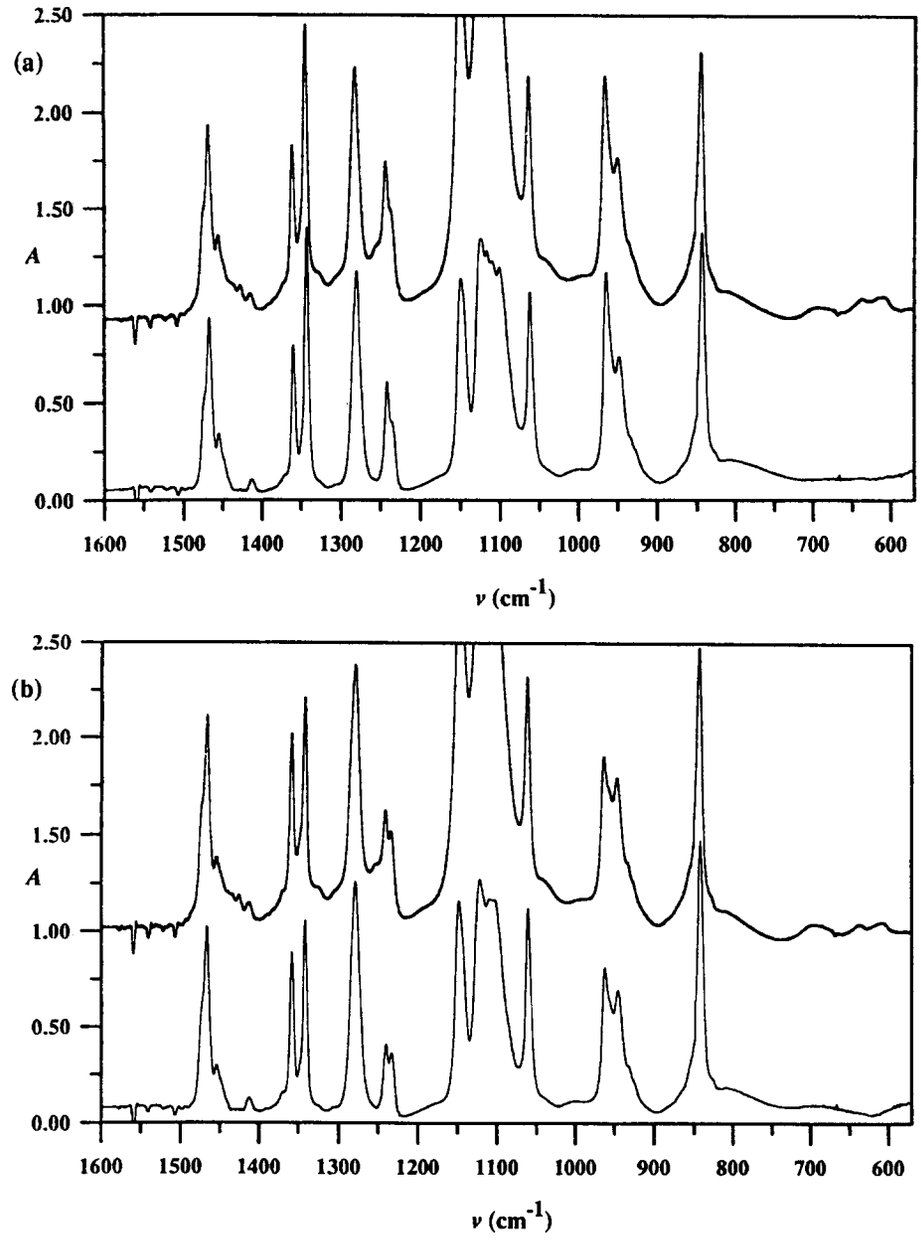

Figure 10 Dichroic spectra of PEO/PVC (75/25), $T_c = 49°C$: (a) parallel spectrum before and after subtraction of the contributions from PVC and amorphous PEO, and (b) perpendicular spectrum before and after difference spectroscopy

PEO/PVC blends. In the case of PEO/PVC blends, the absorbance at 1500 cm^{-1} was used as a baseline reference, and the absorbance difference between two peaks characteristic of PVC at 1427 and 1400 cm^{-1} was used to determine the scaling factor for subtraction of the PVC spectrum. Then the procedure described in the preceding paper[19] for subtraction of the amorphous component of PEO was carried out. As an example, spectra of PEO/PVC (75/25) crystallized at 49°C before and after difference spectroscopy are shown in *Figure 10*.

As shown in *Figure 11*, with increasing concentration of PVC the values of the dichroic ratio for the parallel modes at 1455, 1344, 1243 and 965 cm^{-1} decrease asymptotically to unity. These independent methylene vibrational modes are expected to be the most sensitive to any structural changes. On the other hand, the values of R for the perpendicular modes (i.e., 1468, 1360, 1281 and 1062 cm^{-1}), already close to unity in pure PEO[19], remain unchanged upon addition of PVC, within an experimental uncertainty of $\pm$ 10%. Because $R = 1$ implies an isotropic sample in the plane of the polarizer, it is clear that as the PVC content increases, the arrangement of the crystalline stems becomes increasingly disordered relative to the arrangement in spherulites grown from pure PEO, in accordance with the disordered morphologies observed by PLM. The high sensitivity of the CH_2 wagging mode at 1344 cm^{-1} indicates that the structural changes in PEO involve modifications to the shape of the backbone, i.e., to the polymer conformation, because the wagging mode involves cooperative motion of the methylene carbon atom along the polymer backbone[19]. The increase in the value of R for the representative perpendicular mode at 1468 cm^{-1} with increasing T_c (*Figure 12*) is consistent with the behaviour of pure PEO[20], i.e., a change in the dominant crystal growth face from the (010) to the (120) face. The failure to observe a significant change in the orientation of the parallel bands, such as the representative mode at 1344 cm^{-1} (*Figure 12*), with T_c reflects the fact that these modes are expected to be less sensitive to such a transformation[19]. Apparently the presence of PVC sufficiently perturbs the

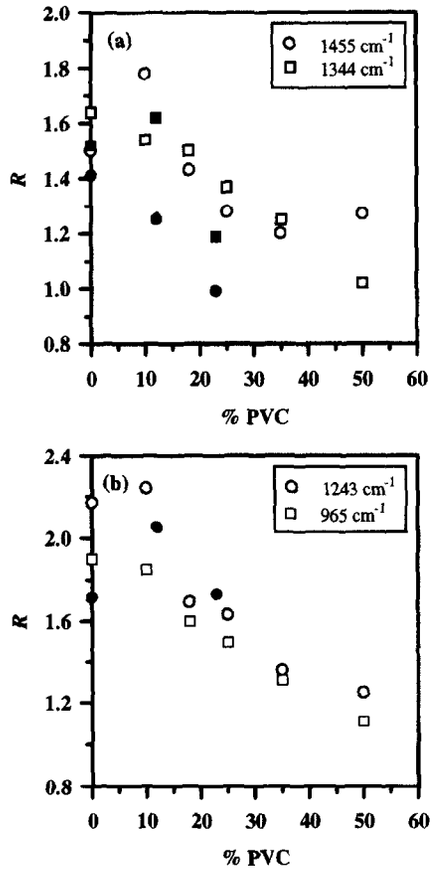

Figure 11 Dichroic ratio, R, of the parallel modes as a function of PVC content, $\Delta T = -2°C$ with respect to the cusp in the growth rate–temperature curve, at (a) 1455 and 1344 cm^{-1}, and (b) 1243 and 965 cm^{-1} (the filled symbols represent data for the TCP mixtures)

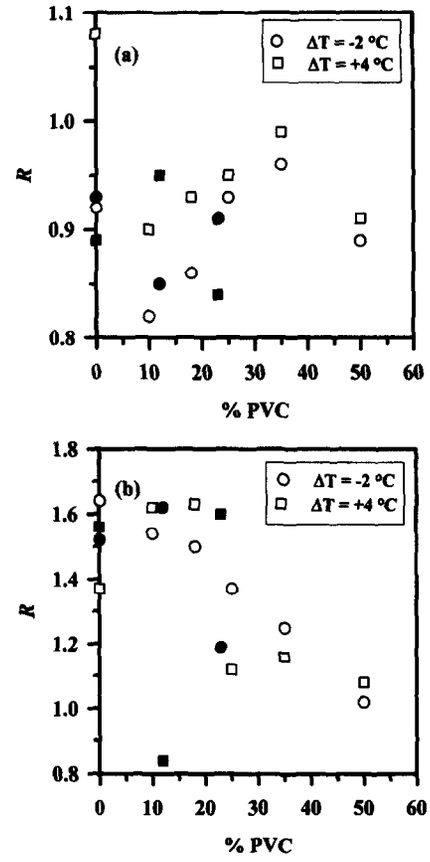

Figure 12 Dichroic ratio, R, for $\Delta T = -2$ and $+4°C$ with respect to the cusp in the growth rate–temperature curve of (a) the perpendicular mode at 1468 cm^{-1} and (b) the parallel mode at 1344 cm^{-1} (the filled symbols represent data for TCP mixtures)

crystalline structure of PEO at the level of the crystalline stems to diminish the observed effect of a change in the growth face.

Because spectra for the individual conformations of PEO are not available, peak ratios where the numerator and the denominator are A values of representative parallel (i.e., planar zig-zag) and perpendicular (i.e., helical) modes, respectively, were used to compare the proportion of the two conformations in the various samples. Plots of A_{1344}/A_{1360}, A_{965}/A_{1062}, A_{1243}/A_{1281} and A_{965}/A_{843} (i.e., $A_{\parallel}/A_{\perp}$) as a function of PEO/PVC blend composition for the perpendicular spectra (*Figure 13*) demonstrate that these peak ratios, and therefore the relative proportion of planar zig-zag conformers, increase with increasing PVC content, within an experimental uncertainty of ± 15%. The parallel components of the spectra show a negligible change relative to each other with changing composition[20]; however, the perpendicular components increase with respect to the parallel components, thereby causing a decrease in the value of R for the predominantly parallel modes. It is likely that the introduction of planar zig-zag segments into the unit cell of PEO is responsible for the diminished effect of the (010)–(120) growth face transition on R data obtained for spherulites grown in PEO/PVC blends. Samples prepared at higher T_c exhibit a significantly lower proportion of planar zig-zag character and similar peak ratio trends. The observed increase in the proportion of the planar zig-zag conformation with increasing PVC content is consistent with the concomitant decrease in the dichroism of PEO. In the process, the overall crystalline order of the spherulite is disturbed.

Tricresyl phosphate mixtures. To separate the PEO crystalline portion from the overall spectra the following

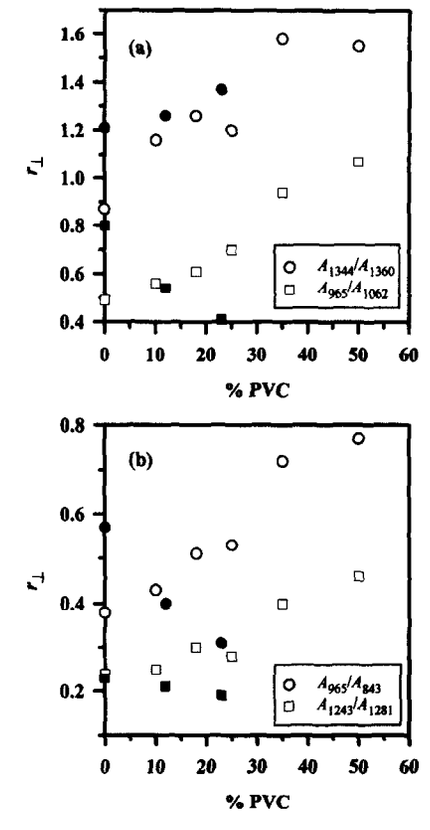

Figure 13 Peak ratio, $r_\perp$, as a function of PVC content, $\Delta T = -2°C$ with respect to the cusp in the growth rate–temperature curve: (a) A_{1344}/A_{1360} and A_{965}/A_{1062}, (b) A_{1243}/A_{1281} and A_{965}/A_{843} (the filled symbols represent data for TCP mixtures).

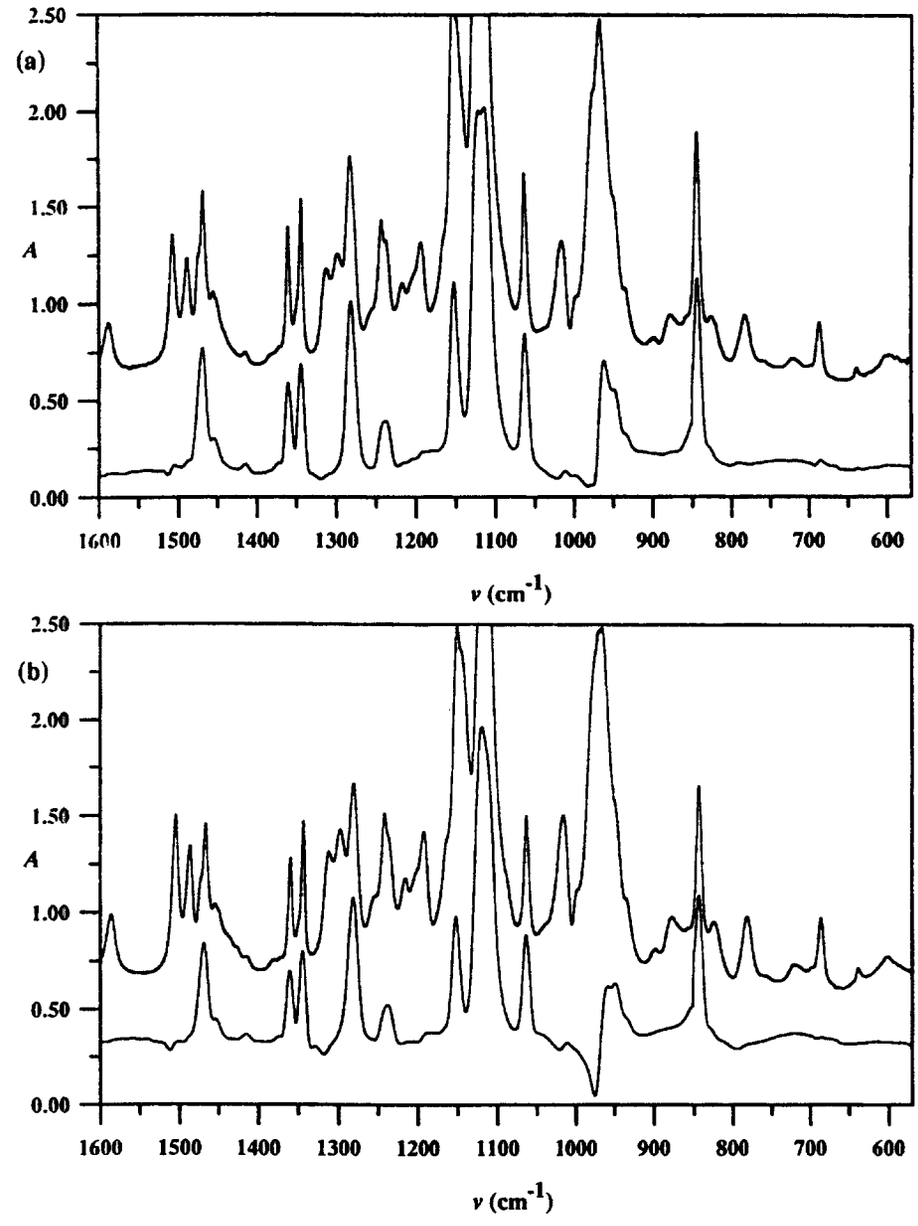

Figure 14 Original and difference spectra for (a) PEO/TCP (67/33), T_c = 40°C, and (b) PEO/PVC/TCP (44/23/33), T_c = 38°C

procedure was used. The contributions of TCP were removed by subtraction using the absorbance at 1550 cm^{-1} as a baseline reference and the area between 1625 and 1565 cm^{-1} as the area for determination of the scaling factor. The contributions arising from PVC and amorphous PEO were then subtracted according to the procedure described in the preceding section. Sample original and difference spectra are given in *Figure 14*. In cases where the high intensity TCP peak between 950 and 1000 cm^{-1} was slightly off-scale, as in *Figure 14*(b), subtraction of this peak led to a negative peak in the resultant difference spectrum. Data from this portion of the spectrum were not employed in the subsequent analysis.

In *Figure 11* the dichroic ratio data are shown for the crystalline PEO peaks at 1455, 1344 and 1243 cm^{-1} in PEO/TCP crystallized at T_c = 40°C and the ternary mixture crystallized at 38°C, i.e., an undercooling of 2°C with respect to the temperature of the cusp in the logarithmic growth rate-temperature plots [*Figure 8*(b)] and the (010)–(120) growth face transition[20]. For PEO/TCP the values of R are generally slightly lower than the corresponding values for pure PEO (T_c = 49°C), indicating a slight perturbation of the crystalline structure by TCP. On the other hand, the data for the peaks at 1344 and 1243 cm^{-1} in PEO/PVC/TCP (55/12/33) samples are similar to those obtained for pure PEO, as is the case for other parallel modes with the exception of the CH_2 bending mode at 1455 cm^{-1}, which exhibits a significant decrease in R. The decrease in R at 1455 cm^{-1} is more pronounced in the case of PEO/PVC/TCP (44/23/33), which contains a larger proportion of PVC relative to the amount of plasticizer.

Peak ratio data for perpendicular spectra of samples containing TCP (ΔT = − 2°C), shown in *Figure 14*, are generally similar to corresponding data for PEO. The proportion of the planar zig-zag conformation in the two ternary mixtures is generally the same as that in pure PEO. Thus, the plasticization of PVC by TCP reduces the effects of PVC on the crystalline structure of PEO.

Conformation of poly(vinyl chloride). Because the interaction between PEO and PVC induces conformational changes in PEO, the question arises as to whether or not

Table 4 Dichroic ratio and peak ratio data for PVC-containing samples and a solution-cast PVC film. (The peak ratios given correspond to parallel spectra)

	R_{615} (*tttt*)	R_{638} (*tttt*)	R_{695} (*tgtg*)	A_{615}/A_{695} (*tttt*/*tgtg*)	A_{638}/A_{695} (*tttt*/*tgtg*)
PEO/PVC					
82/18	0.20	0.29	0.48	0.47	0.71
75/25	1.62	1.56	1.08	1.52	1.44
65/35	1.12	1.12	0.89	1.84	1.70
50/50	0.90	0.91	1.07	1.17	1.21
PEO/PVC/TCP					
55/12/33	2.17	14.2	0.18	8.87	10.5
44/23/33	13.7	3.19	1.85	1.04	1.47
PVC film					
	1.11	1.10	1.00	1.44	1.39

the conformation of PVC is affected in the process as well. The dependence of the vibrational spectrum of PVC on the distribution of different conformations of PVC has been characterized in detail[49–54]. For example, the modes at 615, 638 and 695 cm^{-1} arise from the C–Cl vibrations associated with short *tttt* sequences in syndiotactic segments, longer *tttt* sequences in syndiotactic segments, and *tgtg* sequences in isotactic segments, respectively[49]. Such modes can be used to ascertain the segmental orientation of PVC in oriented samples, as was demonstrated in a recent study of PVC/poly(α-methyl-α-n-propyl-β-propiolactone) blends[55].

The dichroic ratio data for the C–Cl vibrations seen at 615, 638 and 695 cm^{-1} for the samples containing PVC and a reference, solution-cast film are summarized in *Table 4*. The film exhibits a slight degree of orientation from the casting procedure, as expected[51]. As compared to the solution-cast film the modes in the PEO/PVC blends exhibit significant orientation, i.e., values of R that are significantly greater than or less than unity. As the PVC content in the blends increases, the direction of orientation of the C–Cl bonds associated with *tttt* sequences changes from an initial, predominantly radial orientation, as indicated by $R < 1$, in PEO/PVC (82/18) to a tangential orientation (i.e., $R > 1$) in PEOIPVC (75/25), then becomes isotropic in PEO/PVC (65/35). The effect of PEO on PVC is diminished by the lower relative concentration of PEO. The behaviour of the C–Cl bonds associated with *tgtg* sequences follows a slightly different but somewhat similar pattern. The peak ratios listed in *Table 4* demonstrate an increase in the proportion of *tttt* sequences relative to *tgtg* sequences with sample composition. The peak ratios increase dramatically from the 82/18 blend to the 65/35 blend, then decrease in the 50/50 blend. As the PVC molecules come into contact with the advancing, crystallizing front, the rigid nature of the effectively planar growth front promotes the formation of the oriented, planar *tttt* conformation in the strained, amorphous chains.

Although the results for the TCP mixtures are subject to greater uncertainty, due to the spectral subtraction of a TCP peak of similar magnitude to the C–Cl peaks in the complex C–Cl vibrational region, the vibrations in the TCP mixtures are highly oriented, as shown by $R \gg 1$, and $R = 0.18$ in the case of R_{695} for PEO/PVC/TCP (55/12/33). The ratio of *tttt* to *tgtg* is very high in PEO/PVC/TCP (55/12/33) relative to that in PEO/PVC/TCP (44/23/33) due to the larger proportion of TCP relative to PVC in the former mixture. Because the plasticization of PVC by TCP increases the flexibility of the PVC molecules, the influence of the crystallizing PEO on the conformation of PVC will be much greater than the opposite interaction. In effect, the conformation of PEO is perturbed only to a small degree by the additives in these mixtures, as discussed earlier; however, the relatively rigid, planar crystallizing front has a substantial impact on the plasticized PVC molecules that it confronts.

The concomitant tendency towards an increased formation of the planar zig-zag conformation in both PEO and PVC may be a cooperative effect. That is, when both polymers are strained at an interface, their respective conformations are deformed in a manner that readily accommodates both species at the interface. In addition, such adaptation on the part of the PVC molecules need not necessarily be confined to syndiotactic sequences. Molecular modelling studies have demonstrated the potential for isotactic sequences to emulate the shape of the *tttt* conformation[56]. The occurrence of this type of epitaxial effect, which involves mainly interfibrillar PVC, strongly suggests the incidence of cooperative crystallization between the spherulite fibrils, or highly specific orientation between the fibrils.

CONCLUSIONS

The influence of PVC on the crystalline structure of PEO is the determining factor in the slight melting temperature depression observed in PEO/PVC, and not the limited miscibility of PVC and the PEO melt. The addition of TCP plasticizer may cause a small depression in the T_m° of PEO; however, this depression lies within the experimental uncertainty. The plasticizer suppresses the lamellar thickening of PEO substantially through the inclusion of the small molecules in the amorphous fold surfaces of the crystalline lamellae. In fact, this marked interference of TCP in the lamellar thickening of PEO appears to interfere with the determination of accurate values of T_m° in mixtures containing plasticizer.

In general, spherulites grown in the presence of additives are coarser and less birefringent than those grown in the pure melt, with the degree of coarseness increasing with increasing additive concentration. The incidence of banding in spherulites grown in mixtures containing TCP provides further evidence that the plasticizer molecules are included in interlamellar as well as interfibrillar and interspherulitic regions; while the much larger, entangled PVC molecules are included predominantly in the latter two regions. The radial growth rates of PEO spherulites are not affected by the presence of PVC in the temperature

range 49–55°C, even at concentrations as high as 50% PVC. In contrast, the growth rates are severely depressed by the presence of TCP. The anomalous increase in $\sigma\sigma_e$ caused by TCP appears to reflect an increase in σ_e, due to the energetically unfavourable entrapment of TCP molecules within the fold surfaces of the PEO lamellae. However, it is more probable that T_m° data obtained for the TCP mixtures by the Hoffman–Weeks method are significant overestimates of the actual values, and that $\sigma\sigma_e$ remains constant or even decreases slightly.

Dichroic infrared microspectroscopy data indicate that the addition of PVC disturbs the orientation of the crystalline PEO stems within the spherulites and causes an increase in the strained, planar zig-zag conformation. PEO, in turn, induces a higher incidence of the planar zig-zag conformation in the PVC molecules due to epitaxial interaction in interfacial zones between the two polymers. This behaviour strongly suggests the occurrence of cooperative crystallization between spherulite fibrils or specific orientation of the fibrils.

In contrast, TCP does not exert a significant influence on the arrangement of the crystalline stems; nor does it have a significant effect on the chain conformation of PEO. In the ternary mixtures, the plasticizing effect of TCP on PVC renders the PVC molecules more flexible and more mobile, thereby drastically reducing the shearing of PEO and the resultant formation of the planar zig-zag conformation during crystallization and promoting an increased incidence of the planar zig-zag conformation in the PVC molecules. In effect, the crystallization kinetics and the basic crystalline structure of PEO can be controlled by the selection of appropriate proportions of PVC and TCP.

ACKNOWLEDGEMENTS

Financial support in the form of operating grants and postgraduate fellowships (JMM) from the Natural Sciences and Engineering Research Council, Canada and les Fonds pour la Formation et l'Aide à la Recherche (Fonds FCAR) of Quebec, is gratefully acknowledged.

REFERENCES

1. Utracki, L. A., *Polymer Alloys and Blends*. Hanser, New York, 1989.
2. Avella, M., Martuscelli, E. and Greco, P., *Polymer*, 1991, **32**, 1647.
3. Quintana, J. R., Cesteros, L. C., Peleteiro, M. C. and Katime, I., *Polymer*, 1991, **32**, 2793.
4. Martuscelli, E., Silvestre, C. and Gismonde, C., *Makromol. Chem.*, 1985, **186**, 2161.
5. Iriarte, M., Iribarren, J. I., Exteberria, A. and Iruin, J. J., *Polymer*, 1989, **30**, 1160.
6. Cesteros, L. C., Quintana, J. R., Rodriguez Caneiro, M. and Katime, I., *Brit. Polym. J.*, 1989, **21**, 487.
7. Privalko, V. P., Petrenko, K. D. and Lipatove, Yu. S., *Polymer*, 1990, **31**, 1277.
8. Younes, H. and Cohn, D., *Eur. Polym. J.*, 1988, **24**, 765.
9. Nakafuku, C. and Sakoda, M., *Polym. J.*, 1993, **25**, 909.
10. Alfonso, G. C. and Russell, T. P., *Macromolecules*, 1986, **19**, 1143.
11. Cimmino, S., Martuscelli, E. and Silvestre, C., *J. Polym. Sci. Polym. Phys. Ed.*, 1989, **27**, 1781.
12. Martuscelli, E., Pracella, M. and Yue, W. P., *Polymer*, 1984, **25**, 1097.
13. Calahorra, E., Cortazar, M. and Guzman, G. M., *Polymer*, 1982, **23**, 1322.
14. Cimmino, S., Martuscelli, E. and Silvestre, C., *Makromol. Chem., Macromol. Symp.* , 1988, **16**, 147.
15. Chu, E. Y., Pearce, E. M., Kwei, T. K., Yeh, T. F. and Okamoto, Y., *Makromol., Chem. Rapid Commun.*, 1991, **12**, 1.
16. Iragorri, J. I., Cesteros, L. C. and Katime, I., *Polymer Int.*, 1991, **25**, 225.
17. Margaritis, A. G. and Kalfoglou, N. K., *J. Polym. Sci., Polym. Phys. Edn.*, 1988, **26**, 1595.
18. Martuscelli, E., *Polym. Eng. Sci.* , 1984, **24**, 563.
19. Marentette, J. M. and Brown, G. R., *Polymer*, 1998, **39**, 1405.
20. Marentette, J. M., Ph.D. Thesis, McGill University, Montreal, Canada, 1995.
21. Hoffman, J. D. and Weeks, J. J., *J. Res. Natl. Bur. Stand. Sect. A*, 1962, **66**, 13.
22. Afifi-Effat, A. M. and Hay, J. N., *J. Chem. Soc. Faraday Trans. II*, 1972, **68**, 656.
23. Braun, W., Hellwege, K.-H. and Knappe, W., *Coll. Polym. Sci.* , 1967, **215**, 10.
24. Scott, R. L., *J. Chem. Phys.*, 1949, **17**, 279.
25. Flory, P. J., *J. Chem. Phys.*, 1941, **9**, 660.
26. Huggins, M. L., *J. Chem. Phys.*, 1941, **9**, 440.
27. Marco, C., Gomez, M. A., Fatou, J. G., Exteberria, A., Elorza, M. M. and Iruin, J. J., *Eur. Polym. J.*, 1993, **11**, 1477.
28. Czekaj, T. and Kapko, J., *Eur. Polym. J.*, 1981, **17**, 1227.
29. Padden, F. P. Jr and Keith, H. D., *J. Appl. Phys.*, 1959, **30**, 1479.
30. Balta Calleja, F. J., Hay, I. L. and Keller, A., *Koll. Z.-Z. Polym.*, 1966, **209**, 128.
31. Delaite, E., Point, J.-J., Damman, P. and Dosiere, M., *Macromolecules*, 1992, **25**, 4768.
32. Damman, P. and Point, J. J., *Macromolecules*, 1995, **28**, 2050.
33. Keith, H. D., Padden, F. J. Jr., and Russell, T. P., *Macromolecules*, 1989, **22**, 666.
34. Keith, H. D. and Padden, F. J. Jr., *J. Appl. Phys.*, 1964, **35**, 1286.
35. Clark, E. J. and Hoffman, J. D., *Macromolecules*, 1984, **17**, 878.
36. Hoffman, J. D., *Polymer*, 1983, **24**, 3.
37. Lauritzen Jr., J. I. and Hoffman, J. D., *J. Appl. Phys.*, 1973, **44**, 4340.
38. Turnbull, D. and Fisher, J. C., *J. Chem. Phys.*, 1945, **17**, 71.
39. Bartczak, Z., Galeski, A. and Martuscelli, E., *Polym. Eng. Sci.*, 1984, **24**, 1155.
40. Boon, J. and Azcue, J. M., *J. Polym. Sci. Part A-2*, 1968, **6**, 885.
41. Runt, J., Miley, D. M., Zhang, X., Gallagher, K. P., McFeaters, K. and Fishburn, J., *Macromolecules*, 1992, **25**, 1929.
42. Saito, H., Okada, T., Hamane, T. and Inoue, T., *Macromolecules*, 1991, **24**, 4446.
43. Hoffman, J. D., *Polymer*, 1985, **26**, 803.
44. Takahashi, Y. and Tadokoro, H., *Macromolecules*, 1973, **6**, 672.
45. Wang, Y. F. and Lloyd, D. R., *Polymer*, 1993, **34**, 2324.
46. Takahashi, Y., Sumita, I. and Tadokoro, H. J., *J. Polym. Sci.* , 1973, **11**, 2113.
47. Marcos, J. I., Orlandi, E. and Zerbi, G., *Polymer*, 1990, **31**, 1899.
48. Ramana Rao, G., Castiglioni, C., Gussoni, M., Zerbi, G. and Martuscelli, E., *Polymer*, 1985, **26**, 811.
49. Compton, D. A. C. and Maddams, W. F., *Appl. Spectrosc.*, 1986, **40**, 239.
50. Theodorou, M. and Jasse, B., *J. Polym. Sci., Polym. Phys. Ed.*, 1983, **21**, 2263.
51. Chartoff, R. P., Lo, T. S. K., Harrell, E. R. Jr and Roe, R. J., *J. Macromol. Sci., Phys.*, 1981, **B20**, 287.
52. Koenig, J. L. and Antoon, M. K., *J. Polym. Sci., Polym. Phys. Edn.*, 1977, **15**, 1379.
53. Krimm, S., Folt, V. L., Shipman, J. J. and Berens, A. R., *J. Polym. Sci., Part A*, 1963, **1**, 2621.
54. Gilbert, M., *J. Macromol. Sci., Rev. Macromol. Chem. Phys.*, 1994, **C34**, 77.
55. Chabot, P., Prud'homme, R. E. and Pezolet, R. E., *J. Polym. Sci., Polym. Phys. Ed.*, 1990, **28**, 1283.
56. Hobson, R. J. and Windle, A. H., *Polymer*, 1993, **34**, 3582.